Separation Science and Technology
Publication details, including instructions for authors and subscription information:
http://www.informaworld.com/smpp/title~content=t713708471

Purification of Brown Cane Sugar Solutions by Ultrafiltration with Ceramic Membranes: Investigation of Membrane Fouling

S. Jacob[a]; M. Y. Jaffrin[ab]
[a] UMR 6600, DEPARTMENT OF BIOLOGICAL ENGINEERING, TECHNOLOGICAL UNIVERSITY OF COMPIEGNE, COMPIEGNE, FRANCE [b] Institut Universitaire de France,

Online publication date: 16 May 2000

To cite this Article Jacob, S. and Jaffrin, M. Y.(2000) 'Purification of Brown Cane Sugar Solutions by Ultrafiltration with Ceramic Membranes: Investigation of Membrane Fouling', Separation Science and Technology, 35: 7, 989 — 1010
To link to this Article: DOI: 10.1081/SS-100100206
URL: http://dx.doi.org/10.1081/SS-100100206

SEPARATION SCIENCE AND TECHNOLOGY, **35**(7), pp. 989–1010, 2000

Purification of Brown Cane Sugar Solutions by Ultrafiltration with Ceramic Membranes: Investigation of Membrane Fouling

S. JACOB and M.Y. JAFFRIN*
UMR 6600
DEPARTMENT OF BIOLOGICAL ENGINEERING
TECHNOLOGICAL UNIVERSITY OF COMPIEGNE
BP 20529, 60205 COMPIEGNE, FRANCE

ABSTRACT

This paper describes the purification and decoloration of brown cane sugar solutions by ultrafiltration with multichannel 2.5 mm inner diameter ceramic membranes of 15 kDa cutoff. Filtration tests were carried out at concentrations of 30, 40, and 50°Brix, a temperature of 60°C, and 3 and 5 m/s velocities. The permeate flux at 100 kPa decays continuously during 8 hours, reaching at the end 20 L/h·m^2 at 30°Bx and 6 L/h·m^2 at 50°Bx. Higher fluxes were obtained at 300 kPa. The permeate coloration stabilized at 1000 I.U. (ICUMSA units) from a retentate at 2400 I.U., representing a 58% decoloration rate. A comparison was made with microfiltration using a 0.1-μm ceramic membrane. The permeate flux in this case was much higher, decaying from 140 to 100 L/h·m^2 in 8 hours for 30°Bx. In order to reduce membrane fouling, other ultrafiltration tests were performed by superimposing velocity and pressure pulsations of 1 Hz frequency at the membrane inlet. A gain in permeate flux became significant (20%) after 3 hours of filtration. The permeate coloration was not augmented by the pulsations. Attempts to characterize this fouling and to determine its origin were made by comparing the variation of permeate flux or filtered volume versus time with existing fouling models. Best fits were achieved with cake filtration and pore narrowing models.

Key Words. Brown sugar; Ultrafiltration; Membrane fouling; Models

* To whom correspondence should be addressed. Member of Institut Universitaire de France. E-mail: michel.jaffrin@utc.fr

INTRODUCTION

The manufacturing of white sugar requires two successive processes: first sugar extraction from cane or beets, which yields a brown sugar juice, then purification and decoloration to obtain white sugar. These impurities mainly consist of natural polysaccharides (gums) or dextrans produced by microbial infection of damaged cells, and of phenol compounds which are responsible for the color of brown sugar (1). The first process includes several steps of clarification, lime treatment, and crystallization (2). The second process, which is carried out in refineries, includes lime treatment, filtration, decoloration by ion-exchange resins, and successive crystallizations. The goal is to remove impurities such as starch vegetal fibers, sand and gums, and to eliminate the brown color. However, the product manufactured by classical techniques still contains various impurities before the ion-exchange step and therefore the resins are rapidly fouled. Thus, treatment by membrane ultrafiltration or microfiltration has been proposed by various authors (3–7) in order to obtain a higher degree of purity and to decrease the number of clarification steps. Kishihara et al. (3) addressed themselves to the extraction process and investigated the ultrafiltration of raw cane juice at 21.7 Brix units (°Bx). They tested the effect of various pretreatments and compared the efficiency of various organic membranes of cutoff ranging from 5,000 to 30,000 Da. Liming was found to be the most effective pretreatment. Membranes of 10,000 to 30,000 Da were found to be the most suitable for purification but the largest permeate flux (near 100 $L/h \cdot m^2$ at 60°C) was obtained with the 300 kDa membrane. The purity was raised from 90 to 93% and the process was judged superior to the classical lime treatment. Hanssens et al. (4) ultrafiltered raw beet juices using several tubular organic membranes and were able to raise the purity from 87 to 89.4%. Permeate fluxes after 3 hours of filtration were in the vicinity of 50 $L/h \cdot m^2$ at 60°C.

Since sugar filtration can be carried out at high temperatures (80°C), inorganic membranes are well suited for that purpose. Punidadas et al. (5) investigated the purification of brown sugar at 60°Bx with ceramic membranes of various pore sizes from 0.1 to 1.4 μm (Societe des Ceramiques Techniques, Tarbes, France). They used velocities of 5 and 8 m/s with retrofiltration every 3 minutes. When the pore size was increased, the initial permeate flux was higher but decayed over a longer period. After 2 hours the best stabilized flux was 50 $L/h \cdot m^2$ with the 1.4-μm membrane and 58 $L/h \cdot m^2$ at 400 kPa with the 0.8-μm membrane. The 0.2- and 0.5-μm membranes yielded the lowest flux. They reported a decoloration of 40% and a quasicomplete elimination of turbidity (0.12 NTU in permeate versus 170 NTU in retentate). In a more recent paper the same group (6) presented a study relative to the coupling of cross-flow filtration with ion exchange for brown sugar purification. The advantage of treatment by microfiltration was to inhibit poisoning of the ion-exchange

resin. By this technique, 88% of coloration was eliminated but the obtained permeate fluxes of 40 $L/h \cdot m^2$ were thought to be too low to make this process economically competitive. However, beet sugar solutions have been reported to show better filterability than cane sugar ones. Permeate fluxes between 50 and 70 $L/h \cdot m^2$ were quoted by Feuerspiel (7) for thick juice (68°Bx).

It appears from these investigations that microfiltration alone is not sufficient to satisfactorily purify brown sugar solutions and that the present permeate fluxes are too low. Therefore, the goals of this paper are to: a) compare the performances of ultra- and microfiltration for brown sugar purification in terms of flux and decoloration; b) investigate the effect of concentration, transmembrane pressure, and velocity on permeate flux; c) determine the mechanisms of membrane fouling by comparison with existing models; and d) explore hydrodynamical means of fouling control.

MATERIAL AND METHODS

Preparation and Characterization of Solutions

Brown sugar was dissolved in 60°C water to the desired concentration, then prefiltered with a 0.1-mm mesh screen and used immediately. Solid matter concentration was measured by a refractometer ATAGO, N type and expressed in Brix units (°Bx), representing the percentage of solids after calibration by distilled water for concentrations below 32% and by NaCl solution at higher concentrations.

The turbidity of solutions was measured by a HACH RATIO turbidimeter and expressed in NTU after calibration using standard formazine samples. Their coloration was evaluated by measuring the absorbance at 420 nm of a diluted sample at 10°Bx with a pH of 7 using a Shimadzu UV-160 spectrophotometer. The initial coloration was about 2400 I.U. (ICUMSA units). The viscosity of sugar solutions was evaluated from a correlation supplied by Decloux (8):

$$\mu = \exp(a + b/T + c/T^2) \tag{1}$$

with, in S.I. units:

$$a = -1.21\text{–}3.41 \times 10^{-2}\,\mathrm{Bx} + 5.97 \times 10^{-3}\,\mathrm{Bx}^2 - 1.66 \times 10^{-4}\,\mathrm{Bx}^3 + 1.69 \times 10^{-6}\,\mathrm{Bx}^4$$

$$b = -1362 + 35.9\,\mathrm{Bx} - 4.61\,\mathrm{Bx}^2 + 0.127\,\mathrm{Bx}^3 - 1.29 \times 10^{-3}\,\mathrm{Bx}^4$$

$$c = 5.04 \times 10^5 - 6612\,\mathrm{Bx} + 971.62\,\mathrm{Bx}^2 - 25.73\,\mathrm{Bx}^3 + 0.26\,\mathrm{Bx}^4$$

where Bx represents the number of Brix units.

For a fixed temperature, viscosity increases rapidly with the concentration above 50°Bx to reach 10^{-2} Pa·s at 60°C and 60°Bx.

Experimental Setup

Ceramic membranes (KERASEP K01 A-W, Orelis, Miribel, France) of 15 kDa (for ultrafiltration tests) and of 0.1 μm nominal pore size (for microfiltration) were used. The filtration units were multitubular modules, 856 mm long with 19 channels of 2.5 mm internal diameter. The filtration bench (Fig. 1) includes a 40 L closed reservoir to limit evaporation and two heat exchangers to maintain the solutions at the required temperature, generally 60°C. The feed flow was circulated by a volumetric pump with adjustable speed into the filtration unit and returned to the tank. The transmembrane pressure was adjusted by a valve on the retentate (V1). Pressures were measured by VALIDYNE pressure transducers placed upstream and downstream of the filtration module as well as on the permeate side. The feed and permeate flow rates were measured by SPECTRAMED medical electromagnetic flowmeters. In addition, the permeate was collected in a vessel placed on a SARTORIUS electronic scale connected to a PC 386 computer, and the permeate flow rate was calculated by deriving the permeate weight with respect to time using standard density tables for sugar solutions. All transducers and flowmeter signals were fed into the computer through an analogic interface.

The membrane hydraulic permeability was measured before each run using a very low fluid velocity. Water was then replaced by a sugar solution at proper temperature. The fluid velocity was adjusted to the desired value while

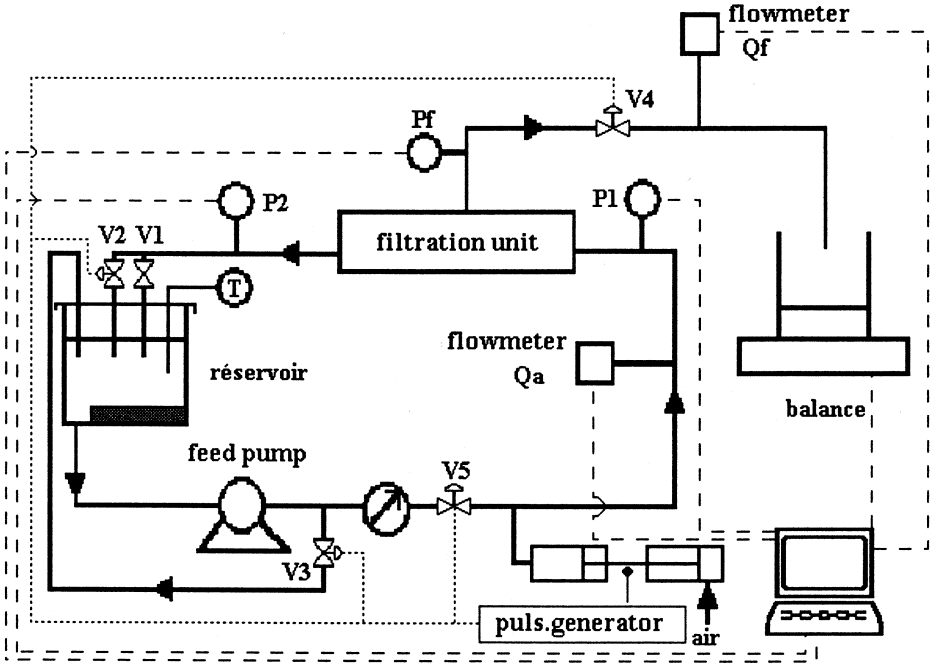

FIG. 1 Experimental batch-type filtration setup with pulsatile generator.

the transmembrane pressure was gradually increased to the target level. After the experiment, membranes were cleaned by circulating 5 L of hot water at 85°C containing 1% of a NaOH solution (HENKEL, P3 ULTRASIL 25F) at low pressure for 2 hours. After rinsing, membrane permeability was measured and, if it was lower than its initial value, the cleaning procedure was repeated. For pulsatile flow tests we added a piston-in-cylinder to the circuit operated pneumatically as in the system of Gupta et al. (9) with adjustable stroke and frequency. It is possible to introduce a retrofiltration in the system by closing valve V5 during the backward stroke of the piston which withdraws flux exclusively from the filtration module, and creates a depression at the retentate side of the membrane.

MODELS OF MEMBRANE FOULING

We summarize here the classical models of membrane fouling under filtration at constant transmembrane pressure described by Hermia (10), which will be compared against our data. The cake filtration model is relevant to external fouling while the others correspond to internal fouling.

Cake Filtration Model

The basic assumption is that the macrosolutes rejected by the membrane form a solid layer or cake with a resistance to filtration R_c increasing proportionally to the amount of volume filtered V_f or, in fact, to the particle mass brought to the membrane by the filtration. Thus, the total filtration resistance may be written

$$R_t = R_{m0} + R_c = R_{m0} + \frac{\alpha C_w V_f}{A_0} \tag{2}$$

where R_{m0} is the membrane resistance, α is the cake specific resistance per unit mass, C_w is the rejected particle concentration near the membrane, and A_0 is the total membrane area. Thus, we may write for the filtration flow rate Q_f:

$$Q_f = \frac{dV_f}{dt} = \frac{P_{tm} A_0}{\mu_f \left(R_{m0} + \dfrac{\alpha C_w V_f}{A_0} \right)} \tag{3}$$

where μ_f is the permeate viscosity. Assuming that R_{m0} and αC_w remain constant, we obtain by integrating Eq. (3):

$$\frac{t}{V_f} = \frac{1}{Q_0} + \frac{\alpha C_w V_f}{2 A_0 R_{m0} Q_0} \tag{4}$$

where $Q_0 = P_{tm} A_0 / \mu_f R_{m0}$ Is the initial permeate flow rate before the cake is formed. On combining Eqs. (3) and (4), another relation for the permeate flow

rate is obtained:

$$\frac{1}{Q_f^2} = \frac{1}{Q_0^2} + \frac{2\alpha C_w t}{A_0 R_{m0} Q_0} \tag{5}$$

Pore Narrowing Model (progressive internal fouling)

This model assumes that a fraction of the microsolute which penetrates inside the pores gets adsorbed on the pore inner surface in such a way that the pore internal volume decays proportionally to Q_f. If L denotes the membrane thickness and N the total number of pores assumed to be cylindrical with uniform radius r, we can write

$$2\pi NLr\frac{dr}{dt} = -CQ_f \tag{6}$$

where C is a dimensionless parameter characterizing the fraction of solute which gets adsorbed. Integration of Eq. (6) with respect to time yields

$$\pi NL(r_0^2 - r^2) = CV_f \tag{7}$$

where r_0 is the initial pore radius. Using Poiseuille's law in the pores and substituting r^2 from Eq. (7), we obtain

$$Q_f = Q_0\left(1 - \frac{CV_f}{V_p}\right)^2 \tag{8}$$

where $V_p = \pi N r_0^2 L$ is the total initial pore volume. Integration of Eq. (8) with respect to time yields

$$\frac{t}{V_f} = \frac{1}{Q_0} + \frac{Ct}{V_p} \tag{9}$$

By combining Eqs. (8) and (9) we obtain

$$\frac{1}{\sqrt{Q_f}} = \frac{1}{\sqrt{Q_0}} + \frac{C\sqrt{Q_0}}{V_p}t \tag{10}$$

Combination of External and Progressive Internal Fouling

Since the sugar solution contains both rejected solutes and microsolutes, a combination of internal and external fouling might be expected. The pore narrowing model amounts to a membrane resistance R_m which increases with time and may be expressed as

$$R_m = \frac{8LA_0}{\pi N r^4} \tag{11}$$

Substituting r^2 from Eq. (7) into Eq. (11), we obtain

$$R_m = R_{m0}\left(1 - \frac{CV_f}{V_p}\right)^{-2} \tag{12}$$

At the beginning of the filtration, if the probability of adsorption is small, the decrease in pore volume is relatively small and Eq. (12) can be approximated by

$$R_m \approx R_{m0}\left(1 + \frac{2CV_f}{V_p}\right) \tag{13}$$

With Eq. (13), Eq. (3) is replaced by

$$Q_f = \frac{P_{tm}A_0}{\mu_f\left[R_{m0} + \left(\frac{\alpha C_w}{A_0} + \frac{2C}{V_p}\right)V_f\right]} \tag{14}$$

Comparison of Eqs. (3) and (14) shows that the contribution of pore narrowing when external fouling is present amounts to an increase in the specific cake resistance. Thus Eqs. (4) and (5) are still valid in this case with a modified value of α, and the contributions of moderate pore narrowing and external fouling cannot be distinguished.

Complete Pore Blocking Model

This is a more drastic form of internal fouling which can occur if particle sizes are equal or close to the pore diameter. This model postulates that a fraction of the pores are completely blocked by particles which penetrate inside the membrane so that the functional area A of the membrane decreases proportionally to the filtered volume:

$$A = A_0 - \sigma V_f \tag{15}$$

where σ is a parameter characterizing the plugging potential of the suspension which can be expected to be proportional to the particle concentration. Here the flux decay is assumed to be solely due to a reduction in membrane area and not to an increase in resistance. The permeate flux is therefore given by

$$Q_f = Q_0\left(1 - \frac{\sigma V_f}{A_0}\right) \tag{16}$$

and by integration of Eq. (16) with respect to time:

$$V_f = \frac{A_0}{\sigma}(1 - \exp(-\sigma J_0 t)) \tag{17}$$

MARCEL DEKKER, INC.
270 Madison Avenue, New York, New York 10016

where J_0 is the initial permeate flux, and by substituting Eq. (17) into Eq. (16):

$$Q_f = Q_0 \exp(-\sigma J_0 t) \quad (18)$$

EXPERIMENTAL RESULTS

Steady Flow Ultrafiltration

First Test

These ultrafiltration tests were carried out at 60°C, a TMP of 100 kPa, a velocity of 5 m/s, and three concentrations of 30, 40, and 50°Bx. The permeate flux decays rapidly (Fig. 2) during the first hour and does not reach a completely stable level even after 8 hours. The permeate fluxes at this point were 20 L/h·m^2 at 30°Bx and 6 L/h·m^2 at 50°Bx. It is interesting to note that, even though the flux values differ significantly for the three concentrations, they decay with time exactly in the same manner (Fig. 3). The variation of the deposited particle layer resistance R_c is plotted as a function of time in Fig. 4. The resistance increases rapidly with time but relatively little with increasing concentration, the resistance at 50°Bx being lower than at 40°Bx. However, when the resistance is plotted as a function of filtered suspended solid mass (the product of filtered volume by the mass concentration) in Fig. 5, the effect of increasing concentration becomes more visible and the resistance at 30°Bx increases less rapidly. A surprising result is the apparent decrease in resistance

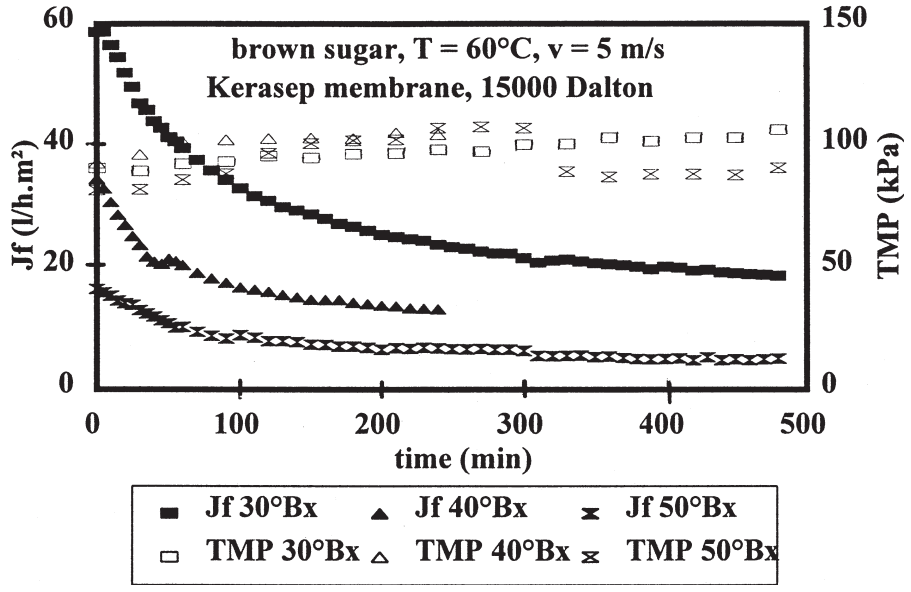

FIG. 2 Permeate flux and transmembrane pressure variations versus time for different solid matter concentrations (membrane cutoff 15 kDa).

MARCEL DEKKER, INC.
270 Madison Avenue, New York, New York 10016

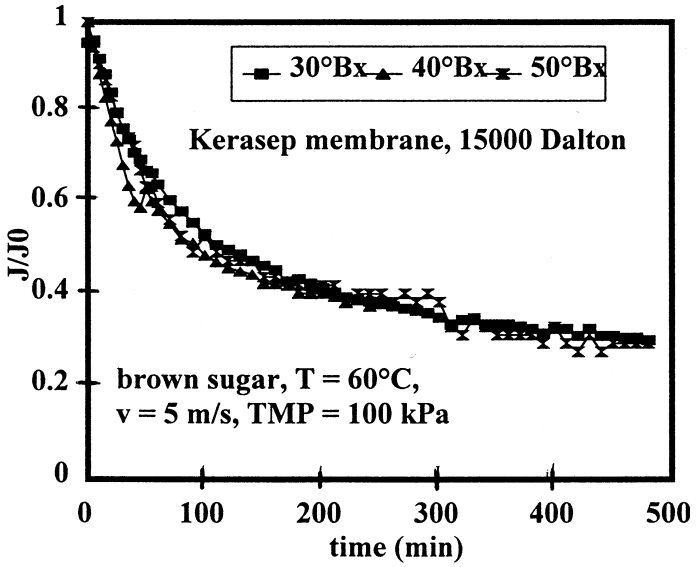

FIG. 3 Variation of permeate flux J/J_0 normalized with respect to its initial value for the same data as Fig. 2.

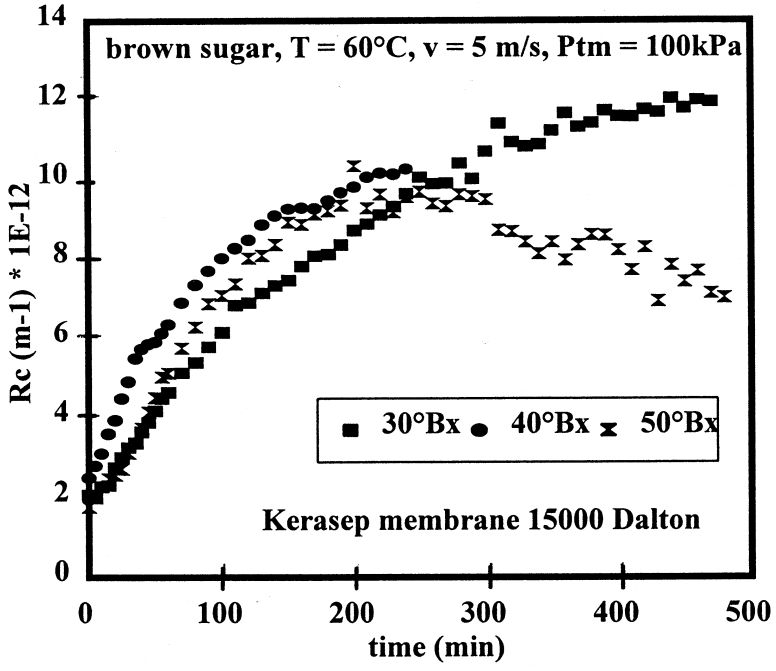

FIG. 4 Variation of cake layer resistance R_c versus time for the same data as Fig. 2.

MARCEL DEKKER, INC.
270 Madison Avenue, New York, New York 10016

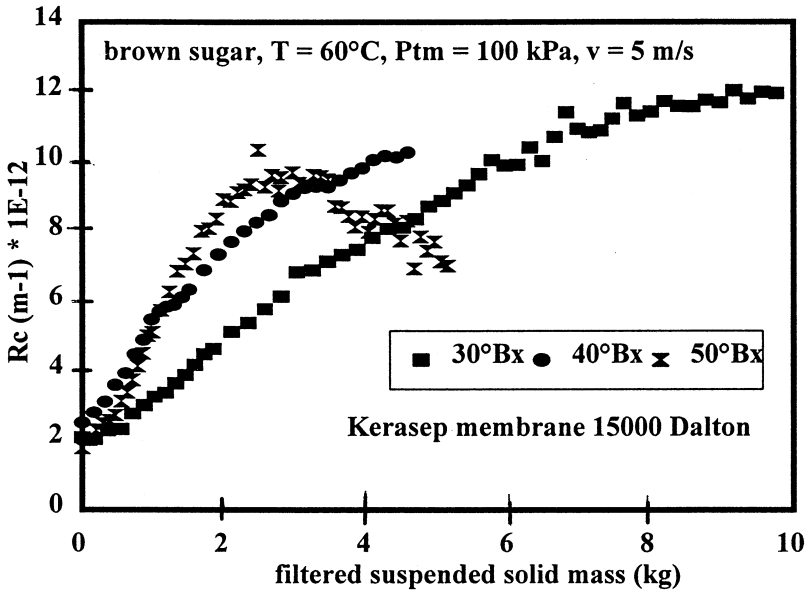

FIG. 5 Variation of cake layer resistance with collected solid mass in permeate for the first UF test.

at 50°Bx when filtered mass exceeds 3 kg. This is caused by a concentration increase from 50 to 56°Bx due to evaporation which increased the permeate viscosity from 3.8 to 6.4 mPa·s.

Second Test

This second test was performed on the same membrane and at the same temperature of 60°C, with a solution at 30°Bx but with a TMP of 300 kPa and a velocity of 3 m/s. Since the lower velocity is compensated by a higher TMP, the variation of permeate flux with time is about the same as in the previous test at the same concentration (Fig. 6). The fluctuations in flux during the first 40 minutes are due to a progressive rise in pressure by 100 kPa increments every 15 minutes. The deposited layer resistance, also shown in Fig. 6, increases faster with time than in the first test, reaching 25×10^{-12} m^{-1} after 6 hours versus 12×10^{-12} m^{-1} in the first test. This is not surprising since the deposited layer can be expected to be thicker at a lower velocity and less permeable at a higher TMP.

The permeate coloration decays from 1700 to 1000 I.U. during the first hour and then increases progressively up to 1300 I.U. at the end of the test. In the first test, this coloration for the concentration of 50°Bx decreases from 1300 I.U. to about 800 I.U. during the first two hours of filtration, and increases also progressively to finally reach almost 1000 I.U. The decoloration rate is shown in Fig. 7 as a function of time for solutions at 30 and 50°Bx.

MARCEL DEKKER, INC.
270 Madison Avenue, New York, New York 10016

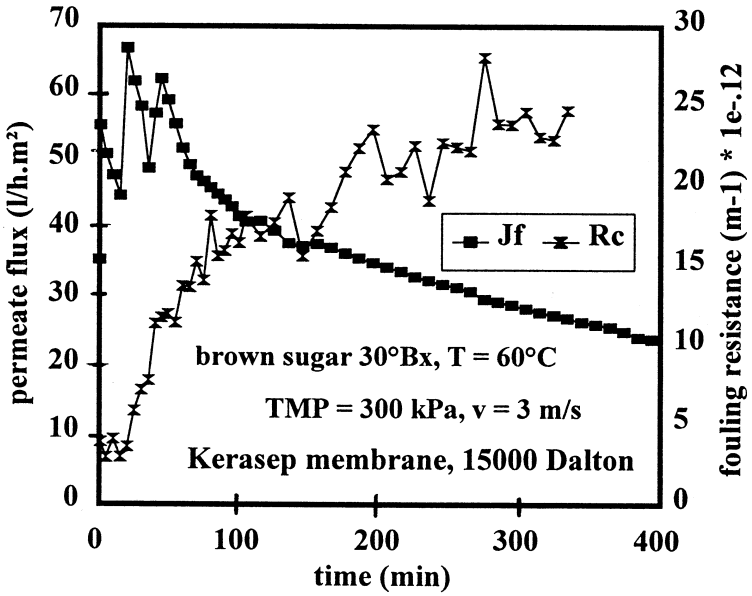

FIG. 6 Variation of permeate flux and cake layer resistance R_c with time for the second UF test (membrane cutoff 15 kDa).

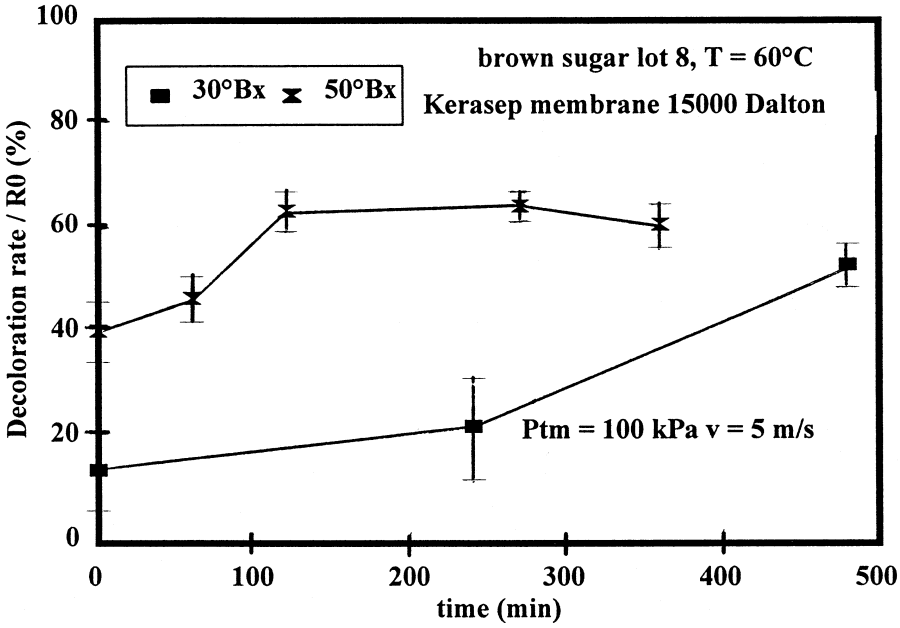

FIG. 7 Percentage rate of decoloration for 30 and 50°Bx solutions as a function of time (first UF test).

MARCEL DEKKER, INC.
270 Madison Avenue, New York, New York 10016

The permeate turbidity drops to about 0.45 NTU from retentate turbidities ranging from 80 to 90 NTU.

Steady Flow Microfiltration

When a 0.1-μm ceramic membrane is used with a 30°Bx solution at the same temperature and the same TMP (100 kPa) and velocity (5 m/s) as in the first test, the permeate flux is found to be much larger than for ultrafiltration (Fig. 8). There is also less flux decay than in ultrafiltration since, after 8 hours, the flux has decreased from 140 to 100 L/h·m^2, a 29% decay instead of 63% for ultrafiltration. However, the permeate flux continues to decrease at a constant rate until at least 8 hours of filtration. These fluxes are higher than those obtained by Punidadas et al. (11) using 0.2 μm ceramic membranes. The additional resistance due to deposited particles increases with time but remains relatively small and at 1.2×10^{12} m^{-1}. This is about nine times less than for the ultrafiltration membrane. This indicates that the finer particles, which are no longer retained by the membrane, accounted for most of the additional resistance.

Pulsatile Flow

Tests were run for the same fluid as for the sudden pressure increase while recycling both retentate and permeate. The mean transmembrane pressure was

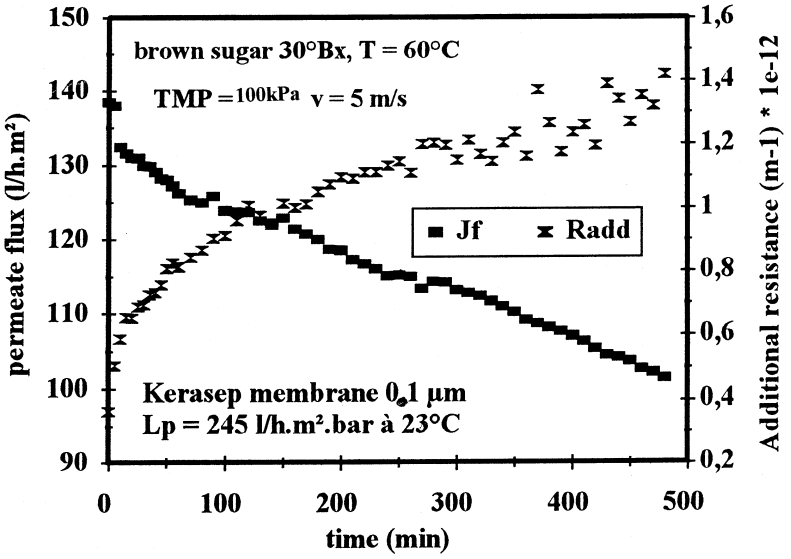

FIG. 8 Variation of permeate flux and additional layer resistance with time for a microfiltration test (0.1 μm pores).

MARCEL DEKKER, INC.
270 Madison Avenue, New York, New York 10016

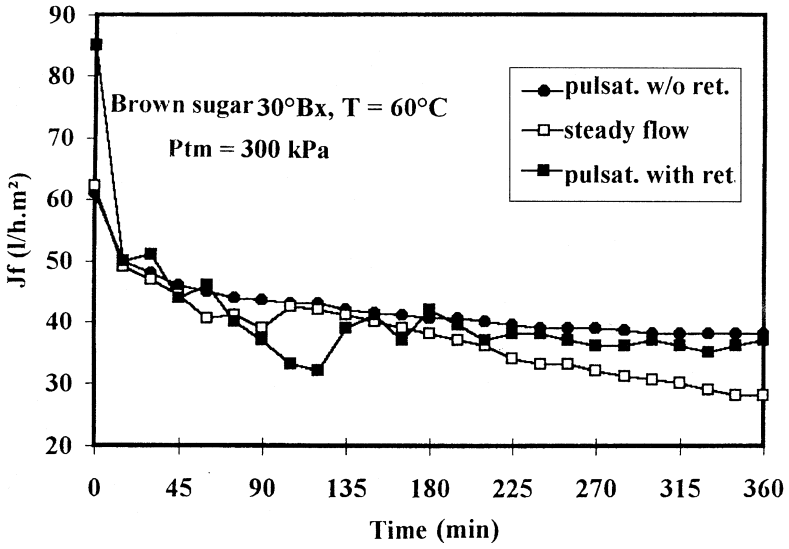

FIG. 9 Comparison of time–mean permeate flux variation for steady and pulsatile flows with and without retrofiltrations (membrane cutoff 15 kDa).

set at 300 kPa which was the value used in steady flow experiments. The TMP varied during a cycle from 100 to 370 kPa while the speed varied from 1.5 to 3.5 m/s. Other experiments were run with retrofiltration during part of the cycle. The TMP varied from −50 to 420 kPa and the speed from −1.3 to 2.5 m/s for a time mean value of 1.7 m/s. The comparison of permeate flux variation with time between steady flow and pulsatile flow experiments is shown in Fig. 9. The benefit of pulsations becomes significant only after about 3 hours of filtration. The presence of retrofiltration does not improve the flux but it must be recalled that the time mean speed was lower (1.7 m/s instead of 3 m/s) in order to avoid excessive pressures. The permeate coloration is not augmented by the presence of pulsations and remained at about 1000 I.U. for a retentate coloration of 3500–3900 I.U.

COMPARISON WITH MEMBRANE FOULING MODELS

In order to test the applicability of the various fouling models to our data, we now present the filtration results of the previous section on steady flow filtration in such a way that agreement between data and the model is represented by a linear correlation. The comparison with the complete pore blocking model is not presented here since the fit was worse than with the other models. The intermediate blocking filtration model which evaluates the probability of a particle to block an open pore was also compared with our data. But this model, which leads to a linear relationship between Q_f^{-1} and time, did

TABLE 1
Determination of Parameter σ and Correlation Coefficients for the Complete Pore Blocking and the Intermediate Blocking Filtration Models

		Complete pore blocking model			Intermediate blocking model		
Test	°Bx	Time interval (minutes)	σ (m^{-1})	r^2	Time interval (minutes)	σ (m^{-1})	r^2
UF1	30	5–40	4.7	0.996	5–50	9.8	0.995
UF1	40	5–35	9.5	0.997	5–40	30.1	0.995
UF1	50	0–55	15.0	0.992	10–50	40.3	0.984
UF2	30	0–20	11.1	0.998	0.20	12.5	0.997

not yield a better fit than the pore blocking model. The results relative to these two models are summarized in Table 1.

Cake Filtration Model

To check the applicability of Eq. (4) on the first ultrafiltration test, we have represented in Fig. 10 the variation of t/V_f versus V_f for the data of Fig. 2 at three concentrations. These variations are reasonably linear as predicted by the model with the correlation coefficients given in Table 2, which are above 0.988 during the first hour. In order to check the consistency of our data with

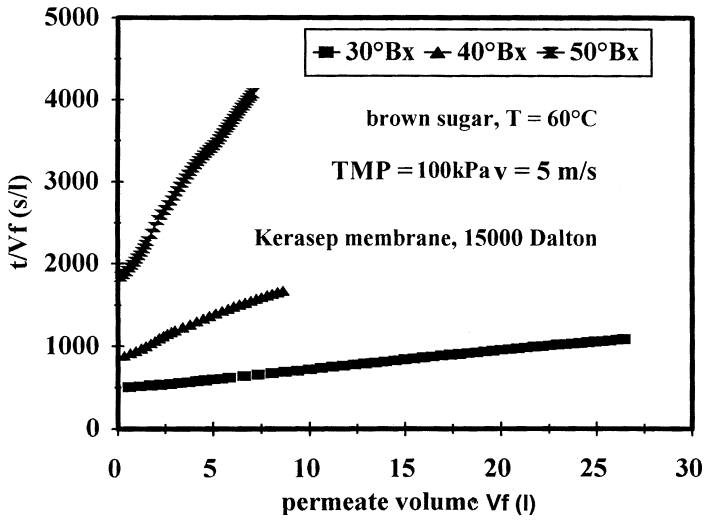

FIG. 10 Variation of t/V_f versus permeate volume V_f to test Eq. (4) of the cake filtration model for the first UF test.

TABLE 2
Determination of Parameter αC_W and Correlation Coefficients r^2 from the Cake Filtration Model for the Two Ultrafiltration Tests

		Equation (4)				Equation (5)			
Test	°Bx	Time interval (minutes)	J_0 (L/h·m^2)	αC_W (m^{-2})	r^2/Fig. number	Time interval (minutes)	J_0 (L/h·m^2)	αC_W (m^{-2})	r^2/Fig. number
UF1	30	0–60	62	3.5×10^{13}	0.995/10	0–60	62	3.6×10^{13}	0.990/11
UF1	40	0–45	36	7.3×10^{13}	0.991/10	0–100	37	8.6×10^{13}	0.983/11
UF1	50	0–60	17	11.8×10^{13}	0.988/10	0–60	18	16×10^{13}	0.965/11
UF2	30	0–30	63	4.6×10^{13}	0.999/12	0–25	63	4.7×10^{13}	0.995/13

Eq. (5) representing the same model, we have plotted the variation of $1/Q_f^2$ with time in Fig. 11. Since the comparison was made on the instantaneous permeate flow Q_f and not on the permeate volume V_f, the linear fit is not as good as in Fig. 10 and the correlation coefficients are slightly lower (0.965–0.99) but still very good. It is interesting to notice that the two correlations of Figs. 10 and 11 using Eqs. (4) and (5), respectively, yield very similar values of αC_w at the same concentration. These values increase with increasing concentration. Figure 5, which shows the variation of the layer resistances with a solid mass collected in permeate, can be regarded as a third test of this model ac-

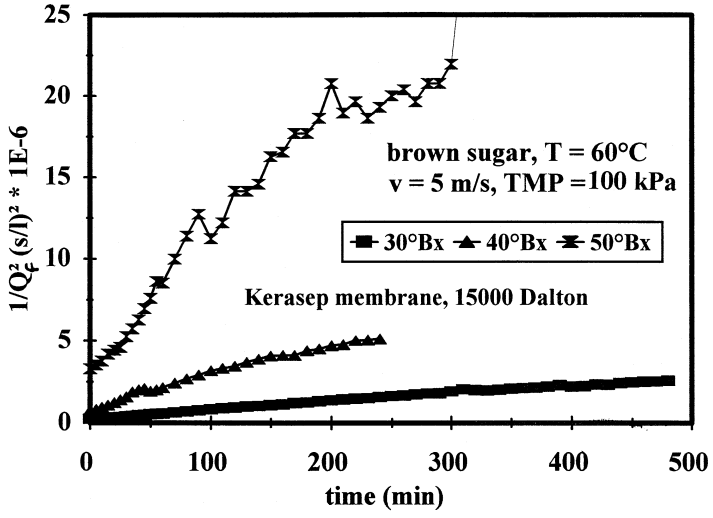

FIG. 11 Variation of $1/Q_f^2$ versus time to test Eq. (5) of the cake filtration model for the first UF test.

MARCEL DEKKER, INC.
270 Madison Avenue, New York, New York 10016

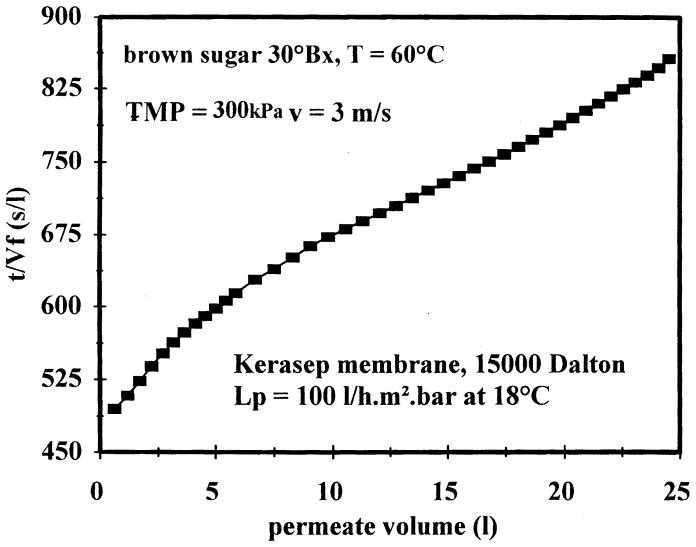

FIG. 12 Variation of t/V_f versus permeate volume V_f to test Eq. (4) of the cake filtration model for the second UF test.

cording to Eq. (2) since this mass is proportional to permeate volume if the sieving coefficient remains constant. It indicates that the rate of growth of the layer resistance decreases slightly after some time. This may be due to increased shear when the cake becomes thick enough to decrease the membrane lumen. The same treatment applied to the second test at 30°Bx is illustrated in Figs. 12 and 13 for t/V_f and $1/Q_f^2$, respectively. The corresponding values of

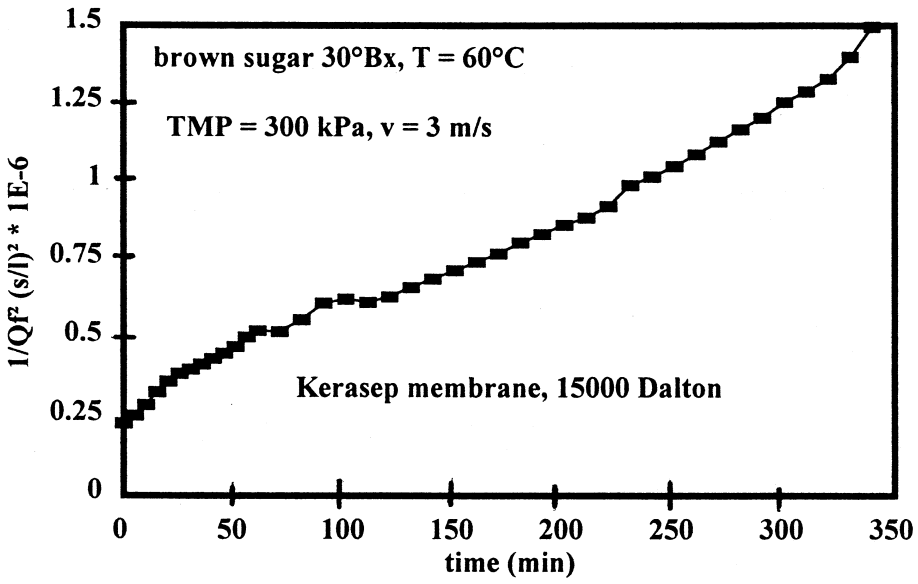

FIG. 13 Variation of $1/Q_f^2$ versus time to test Eq. (5) of the cake filtration model for the second UF test.

αC_w, also shown in Table 2, are close for the two curves and slightly higher than for the first test (4.6×10^{13} instead of 3.5×10^{13} m^{-2}), which is consistent with the higher resistance observed. The linearity of the correlations is very good during the first 30 minutes of filtration with correlation coefficients of 0.999 and 0.995, respectively, for Figs. 12 and 13. After about 2 hours the correlations are again linear, but with a smaller slope.

Pore Narrowing Model

Figure 14 represents the variation of t/V_f for the data of Fig. 2 as a function of time in order to check the agreement with Eq. (9). It can be noticed that the slopes of the curves representing the data decay after the first hour and remain constant after 3 hours. The same observation is even more striking in Fig. 15 which represents $1/\sqrt{Q_f}$ versus time in accordance with Eq. (10). As for the cake filtration model in Fig. 11, the fit with the pore narrowing model at larger times is not as good for the instantaneous permeate flow rate as for the cumulated permeate volume.

Table 3 indicates the values of the constant C/V_p calculated from the experimental data of Fig. 13 using Eq. (9) and of Fig. 14 using Eq. (10). We have computed the value of C/V_p for the 50°Bx curve of Fig. 14, both during the first hour and after 200 minutes. The latter value is about 45% of the first one, indicating a smaller rate of adsorption at large times, which is logical. Here also, it is also interesting to note that the values of C/V_p calculated from the

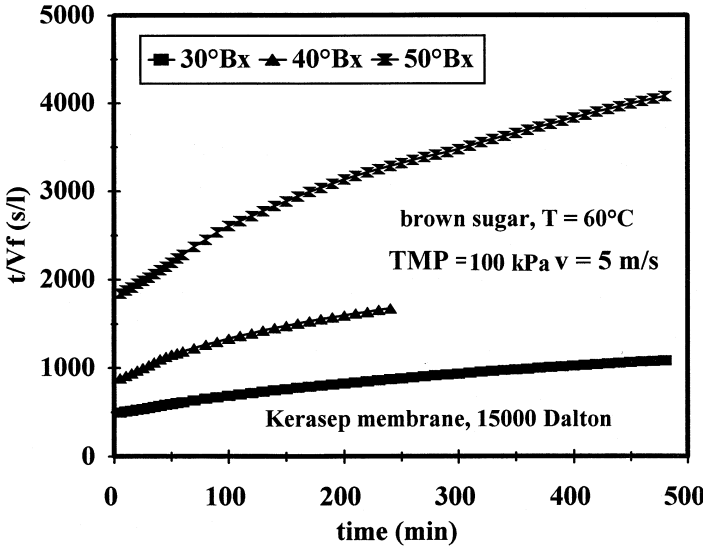

FIG. 14 Variation of t/V_f versus time to test Eq. (9) of the pore narrowing model for the first UF test.

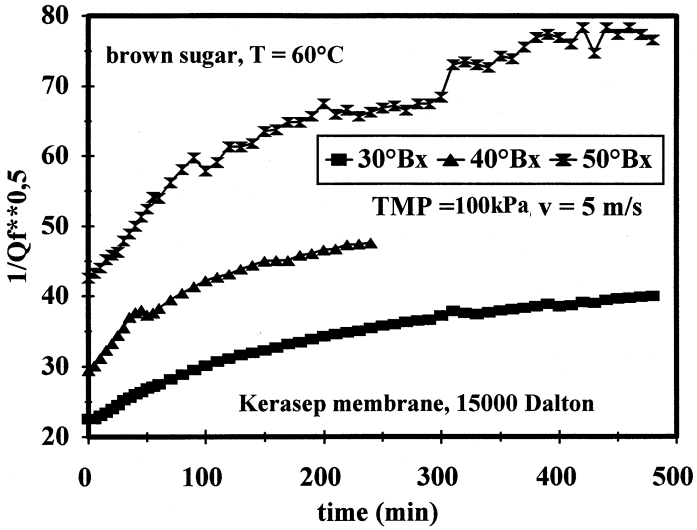

FIG. 15 Variation of $Q_f^{-1/2}$ versus time to test Eq. (10) of the pore narrowing model for the first UF test.

two figures for each concentration are very close and that the probability of adsorption increases with the concentration.

The application of the pore narrowing model to the second ultrafiltration test is illustrated in Fig. 16 using Eqs. (9) and (10). A linear regression is obtained after 2 hours of filtration. It corresponds, as shown in Table 3, to a constant rate of adsorption (C/V_p) of 12 m^{-3} which is significantly less than in the

TABLE 3
Determination of Parameter C/V_p and Correlation Coefficients r^2 from the Pore Narrowing Model for Ultrafiltration and Microfiltration Tests

		Equation (9)				Equation (10)			
Test	°Bx	Time interval (minutes)	J_0 (L/h·m^2)	C/V_p (m^{-1})	r^2/Fig. number	Time interval (minutes)	J_0 (L/h·m^2)	C/V_p (m^{-1})	r^2/Fig. number
UF1	30	5–60	62	36.1	0.999/14	5–60	61	34.3	0.991/15
UF1	40	5–55	35	99.1	0.998/14	5–40	36	107.0	0.997/15
UF1	50	5–55	17	130.0	0.998/14	0–55	17	144.6	0.986/15
UF1	50	200–480	—	56.6	0.999/14	—		—	—
UF2	30	110–350	31	12.5	0.999/16	110–350	49	12.1	0.998/16
MF	30	90–480	132	1.02	0.999/17	90–480	132	1.07	0.990/17

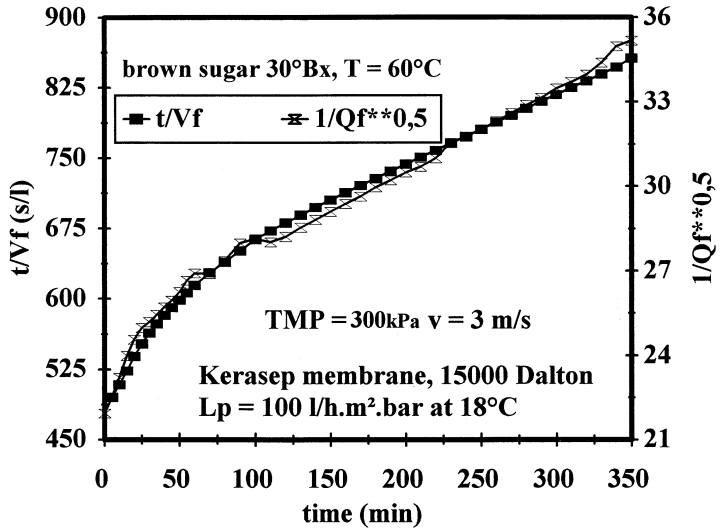

FIG. 16 Application of the pore narrowing model to the second ultrafiltration test using E (9) and (10).

first test at the same concentration (35 m^{-3}). Again, Eqs. (9) and (10) yield virtually the same value of C/V_p.

We have also applied the pore narrowing model to the microfiltration test. The results are displayed in Fig. 17 using Eqs. (9) and (10). A linear fit is obtained for the two curves after 1 hour of filtration. The values of C/V_p (Table 3) are less than one-thirtieth of those obtained in ultrafiltration in the same conditions and are identical for the two equations.

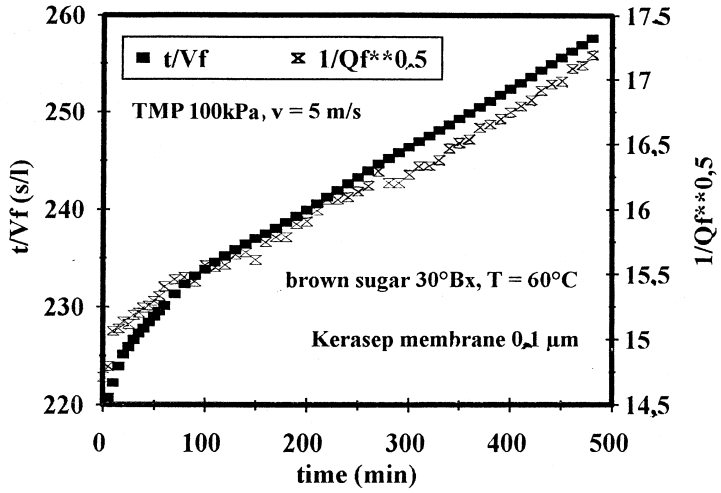

FIG. 17 Application of the pore narrowing model to the microfiltration test using Eqs. (9) and (10).

DISCUSSION AND CONCLUSIONS

Our results confirm those from the literature, namely that permeate fluxes are smaller in ultrafiltration than in microfiltration, but that decoloration is more important. Although our experimental conditions were different from those encountered in industry, the permeate flux measured in our case for 50°Bx should be close to that in industrial conditions (67°Bx) because the effect of lower concentration in our tests is compensated for by a lower temperature (60°C, for safety) than in industry (80°C). The application of pulsations on inlet flow significantly improved the permeate flux after 4 hours of ultrafiltration, but the effect of retrofiltrations was limited. We are therefore led to postulate that fouling during ultrafiltration is for a good part superficial. This conclusion is in agreement with the comparison of our data with fouling models. The cake filtration model (superficial fouling) reproduces satisfactorily the observed variations of t/V_f with V_f and Q_f^{-2} with time for both ultrafiltration tests during the first hour. Moreover, the parameter αC_w inferred from this model, which represents the fouling resistance per unit volume of permeate flux, is independent of the method for its determination and increases with increasing solid matter concentration as expected. Its values are also similar in the two tests. Unfortunately, none of the models tested fitted the data during the entire duration of the tests. Straight lines with different slopes were generally observed during the first hour and at larger times. Internal fouling (pore narrowing model) should not be discounted in ultrafiltration, first because it fits the data during the 5–55 minute interval and second because, as shown in the Models of Membrane Fouling section, it is possible that it occurs together with cake formation without formally affecting the description of the cake filtration model. In the case of microfiltration the cake filtration model was unsatisfactory and therefore it was not presented here. A good fit was obtained with the pore narrowing model, which is logical because internal fouling is more frequent in microfiltration because of the larger pore size.

Although it may seem superfluous, we think that it was worthwhile to use two different equations to check the applicability of the different models. These two equations were not equivalent since one involved the instantaneous permeate flow rate and the other the permeate volume obtained by integration over time. It was indeed comforting to see that these two equations led to similar values of the parameters characterizing the fouling in most cases, and that these parameters varied with operating conditions as expected.

ACKNOWLEDGMENTS

The assistance provided by Dr. Martine Descloux and Laurence Tatoud from ENSIA, Palaiseau, and Patrick Paullier from UTC, as well as the financial support of Orelis Company, Miribel, France, are gratefully acknowledged.

SYMBOLS

A	membrane area (m^2)
C	dimensionless parameter (Eq. 6)
C_w	rejected particle concentration at membrane (kg/m^3)
J	permeate flux ($L/h \cdot m^2$). $1\ L/h \cdot m^2 = 2.78 \times 10^{-7}$ m/s
L	membrane thickness (m)
N	total number of pores in the membrane
P_{tm}	transmembrane pressure (Pa)
Q_f	permeate flow rate (m^3/s)
Q_0	initial permeate flow rate (m^3/s)
r	pore radius (m)
R_c	cake layer resistance (m^{-1})
R_m	membrane resistance (m^{-1})
t	time (s)
V_f	permeate volume (m^3)
V_p	initial total pore volume (m^3)
α	cake specific resistance (m/kg)
μ_f	permeate viscosity (Pa·s)
σ	parameter characterizing plugging potential of suspension (m^{-1})

Subscript

0	initial

Abbreviations

kDa	10^3 dalton
I.U.	ICUMSA units
NTU	turbidity unit

REFERENCES

1. C. P. Chen and C. C. Chou, *Cane Sugar Handbook*, 12th ed., Wiley, Canada, 1993.
2. M. P. Bernardin, *Le sucre*, 6th ed., Centre Etudes et de Documentation du Sucre, Paris, 1984.
3. S. Kashihara, S. Fuji, and M. Komoto, "Ultrafiltration of Cane Juice: Influence of Flux and Quality of Permeate," *Int. Sugar J.*, *83*, 35–39 (1981).
4. T. R. Hanssens, J. G. M. An Vispen, K. Koerts, and L. H. de Nie, "Ultrafiltration as an Alternative for Raw Juice Purification in the Beet Sugar Industry," *Zuckerindustrie 109*, 152–156 (1984).
5. P. Punidadas, M. Decloux, and G. Trystram. "Microfiltration tangentielle sur membrane minérale en céramique: Application au traitement du sucre roux," *Ind. Aliment. Agric.*, pp. 615–623 (July–August 1990).
6. M. Decloux, E. Ben Messaoud, and M. L. Lameloise, "Etude du couplage microfiltration tangentielle/échange d'ions en raffinerie de sucre de canne," *Ibid.*, pp. 495–502 (July–August 1992).

MARCEL DEKKER, INC.
270 Madison Avenue, New York, New York 10016

7. H. S. Feuerspiel, "Ceramic Membrane Filtration Technology in Wet Corn Milling and Sugar Industry," in *Proceedings of the World Congress of Filtration*, Budapest, May 1996, pp. 550–600.
8. M. Decloux, Personal Communication.
9. B. B. Gupta, P. Blanpain, and M. Y. Jaffrin, "Permeate Flux Enhancement by Pressure and Flux Pulsations in Microfiltration with Mineral Membranes," *J. Membr. Sci.*, *70*, 257–266, 1992.
10. J. Hermia, "Constant Pressure Blocking Filtration Laws. Application to Power-Law Non-Newtonian Fluids," *Trans. Inst. Chem. Eng.*, *60*, 183–187 (1982).
11. P. Punidadas and M. Decloux, "Experimental Results of Purification of Sugar Solutions by Cross Flow Filtration on Mineral Membranes," in *Proceedings of the 5th World Filtration Congress*, *Vol. 3*, Nice, France, 1990, p. 284.

Received by editor May 4, 1999
Revision received October 1999

Request Permission or Order Reprints Instantly!